Advances in Aircraft and Spacecraft Science, *Vol. 5, No. 5 (2018) 581-594*
DOI: https://doi.org/10.12989/aas.2018.5.5.581

Effects of chemistry in Mars entry and Earth re-entry

Gennaro Zuppardi*

Department of Industrial Engineering, University of Naples "Federico II" – Aerospace Division
Piazzale Tecchio 80, 80125 Naples, Italy

(Received January 3, 2018, Revised March 18, 2018, Accepted March 21, 2018)

Abstract. This paper is the follow-on of a previous paper by the author where it was pointed out that the forthcoming, manned exploration missions to Mars, by means of complex geometry spacecraft, involve the study of phenomena like shock wave-boundary layer interaction and shock wave-shock wave interaction also along the entry path in Mars atmosphere. The present paper focuses the chemical effects both in the shock layer and on the surface of a test body along the Mars orbital entry and compares these effects with those along the Earth orbital re-entry. As well known, the Mars atmosphere is almost made up of Carbon dioxide whose dissociation energy is even lower than that of Oxygen. Therefore, although the Mars entry is less energized than the Earth re-entry, one can expect that the effects of chemistry on aerodynamic quantities, both in the shock layer and on a test body surface, are different from those along the Earth re-entry. The study has been carried out computationally by means of a direct simulation Monte Carlo code, simulating the nose of an aero-space-plane and using, as free stream parameters, those along the Mars entry and Earth re-entry trajectories in the altitude interval 60-90 km. At each altitude, three chemical conditions have been considered: 1) gas non reactive and non-catalytic surface, 2) gas reactive and non-catalytic surface, 3) gas reactive and fully-catalytic surface. The results showed that the number of reactions, both in the flow and on the nose surface, is higher for Earth and, correspondingly, also the effects on the aerodynamic quantities.

Keywords: hypersonic; rarefied aerodynamics; effects of chemical reactions in Mars entry; effects of chemical reactions in Earth re-entry; direct simulation Monte Carlo method

1. Introduction

The present paper is the follow-on of a paper by the author (Zuppardi 2018) where it was pointed out that the forthcoming manned exploration missions to Mars, by means of complex geometry spacecrafts as per lifting vehicles provided with control aerodynamic surfaces, involve the study of phenomena, typical of hypersonic Aerodynamics such as Shock Wave-Boundary Layer Interaction (SWBLI) and Shock Wave-Shock Wave Interaction (SWSWI) also along the entry path in Mars atmosphere. As well known, the Mars atmosphere is almost made up of Carbon dioxide whose dissociation energy is even lower than that of Oxygen; the dissociation energy of Carbon dioxide is 9.9 MJ/kg, that of Oxygen is 15.5 MJ/kg. Therefore, even though the Mars entry is less energized than the Earth re-entry (the flow energy, at the altitude of 90 km of the orbital entry, is about 10.9 MJ/kg for Mars and about 29.8 MJ/kg for Earth), it has to be expected that the chemical effects on the aerodynamic quantities both in the shock layer and on the surface of a

*Corresponding author, Senior Lecturer, E-mail: zuppardi@unina.it

http://www.techno-press.org/?journal=aas&subpage=7 ISSN: 2287-528X (Print), 2287-5271 (Online)

space vehicle are different from those in Earth re-entry.

When a gas flows around a space vehicle at high velocity, such as that along a planet entry trajectory, it can be characterized by an energy higher than the dissociation energy and even higher than the ionization energy of the molecules of the planet atmosphere. Both ionization and dissociation reactions are beneficial because, being endothermic, they absorb energy from the flow and reduce the heat flux exchanged with the surface of a space vehicle.

Ionization produces protons and electrons, dissociation produces atomic species. These radical species spread in the flow field and some of them reach the space vehicle surface. In space application, the surface of a vehicle must be kept, for structural reason, at "low" temperatures, of order 2000 K at most (Barbato and Bruno 1996). At low surface temperature, the ionized species tend to regain the lost electron (or to de-ionize) and the dissociated species tend to recombine. Both the de-ionization and the recombination reactions are exothermic; this means that these reactions give back the energy used for ionizing and dissociating the molecules in the flow and increase the heat flux to the space vehicle surface. For this reason, one of the most important topic in the current aerospace research is related to the choice of the most proper material for the Thermal Protection System (TPS). In order to efficiently counteract the increase of heat flux due to de-ionization and to recombination, the TPS material has to exhibit a low level of cataliticity.

The problem of aerodynamics and of aerothermodynamics of the Mars atmosphere is very relevant as shown by the literature on the subject. Only to cite some recently published journal articles, the reader can refer to Reynier (2014), Yang *et al*. (2014), Kolesnikov *et al* (2016); the work by Hollis and Prabhu (2013) includes also the boundary layer region, Wang *et al*. (2016) investigate both lamina and turbulent heating, while (Hao *et al*., 2017) emphasize the importance of the evaluation of transport parameters. The aim of the present paper is to quantify the chemical effects in Mars entry and to compare them with those in Earth re-entry and to point out the differences. The present study considers the aerodynamic quantities both in the shock layer (gas composition, temperature and so on) and on the test body surface (pressure, heat flux and so on). This part of the work can be useful for providing information to the designer about the proper project (sizing, choice of material, etc.) of the TPS.

This study has been carried out computationally simulating, as test body, a possible nose of an aero-space-plane. Both the Mars and the Earth computations have been carried out in the altitude interval 60-90 km considering, at each altitude, three chemical conditions: 1) non-reactive gas and non-catalytic surface, 2) reactive gas and non-catalytic surface, 3) reactive gas and fully-catalytic surface. Quantification is fulfilled in terms of the percentage differences of aerodynamic quantities between the chemical conditions.

Previous computations (Zuppardi *et al*. 2014) verified that the maximum value of heat flux, at the nose stagnation point of SpaceLiner, is met at altitudes close to these altitudes. The nose simulated in the present tests is axis-symmetric and its dimension (base diameter) is such that the flow field in the altitude interval is in continuum, low density regime therefore using a direct simulation Monte Carlo code has been mandatory.

2. Direct simulation Monte Carlo method and DS2V-64bits code

The Direct Simulation Monte Carlo (DSMC) method (Bird 1998, Bird 2013, Shen 2005) is a computational, statistical and stochastic method, solving flow fields from the free molecule regime to the continuum low-density regime. DSMC relies on the kinetic theory of gases and considers

the gas as made up of millions of simulated molecules, each one representing a large number of real molecules (in the present computations of the order of 10^9) in the physical space.

The evolution of molecules, in terms of velocity, spatial coordinates and internal thermodynamic/chemical status, is produced by intermolecular collisions and molecule-surface interactions within the simulated physical space. This is divided into cells both for selecting the colliding molecules and for sampling the thermo-fluid-dynamic quantities. The molecules in a cell represent those at the same location in the physical field. The method does not rely on integration of differential equation therefore it does not suffer from numerical instabilities but it is inherently unsteady with a steady solution achievable after a sufficiently long simulation time.

The basic assumption of the method is the temporal decoupling of motion and collision of the simulated molecules. The motion and collision phases are computed by two distinct algorithms, performed sequentially. This assumption holds when the evolution time step of the aerodynamic system (or global time step), is shorter than the collision time or the time between two subsequent molecular collisions. In the motion phase, the simulated molecules move ballistically at their velocity over the global time step. Molecules change position in the flow field and interact with the surface of the body under study. In the collision phase, a couple of colliding molecules are selected in the computing cell. Chemical reactions take place, both colliding molecules exchange energy among the translational and interior degrees of freedom (rotation, vibration) and change velocity. The macroscopic gas properties (density, temperature, etc.), the aerodynamic force and the heat flux, exchanged with the body surface, are computed by sampling molecular quantities (number density, gas composition, momentum, kinetic energy, internal energy, etc.) over a pre-fixed number of global time steps.

The DSMC code used in the present study is the general 2D/axisymmetric code DS2V-4.5 64bits (Bird 2012). DS2V-4.5 64bits is "sophisticated"; a DSMC code is defined sophisticated if it implements computing procedures achieving both greater efficiency and accuracy with respect to a "basic" DSMC code. More specifically, a sophisticated code (Bird 2006, Bird *et al.* 2009, Gallis *et al.* 2009):

1) divides the computational volume into two grids or sets of cells (collision and sampling) with the related cell adaptation. The DS2V-4.5 64bits code automatically generates the number of cells and the structure of the collision and sampling grids on the basis of the input megabytes (1300 in the present computations) and of the free stream number density. However, the user can change the number of cells and therefore the structure of grids by inputting the number of molecules for the adaptation of the collision and of the sampling cells; the lower the input number of molecules per cell, the higher the number of cells after the adaptation process,

2) implements the "nearest neighbor" procedure for the selection, in the collision cell, of the pair of colliding molecules. This procedure is aimed at fulfilling the physical condition that a molecule collides with the molecule closest to it. This implies that, when a molecule is chosen at random in the collision cell, the collision partner is the molecule closest to it. In the "basic" DSMC method, the collision partner was selected at random in the same computing cell.

3) provides an optimal global time step. This is computed as a fraction (say 0.2) of the current, average collision time over the computing dominion. In the "basic" DSMC method, the global time step was an input to the code and then kept constant during the evolution of the system, therefore irrespective of the actual, evolving fluid-dynamic conditions.

4) avoids sequential collisions between the same collision pair. This procedure avoids a second collision between the same collision partners; this is physically impossible because after a collision, the molecules move away in opposite directions.

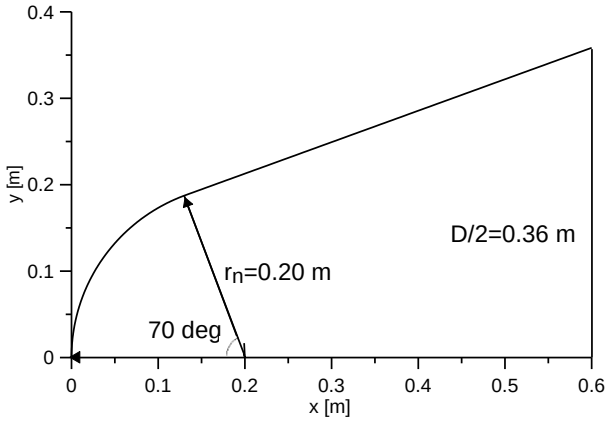

Fig. 1 Test body

5) allows the user to evaluate the quality of the computation by means of the evaluation of the adequacy of the number of simulated molecules. The ratio between the molecule mean collision separation (mcs) and the mean free path (λ), in each collision cell, is the parameter making possible this evaluation; mcs/λ has to be less than unity everywhere in the computational domain for a good quality of a DSMC computation. Bird (2006) suggests that the mcs/λ ratio should be less than 0.2 for an optimal quality of the computation.

Finally, DS2V-4.5 64bits provides indication also about the stabilization of the DSMC computation. This is achieved when the profile of the simulated molecules, as a function of the simulated time, becomes jagged and included within a band which defines the standard deviation of the number of simulated molecules.

3. Test conditions

Figure 1 shows the axial-symmetrical test body, representing the nose or the first part (0.60 m) of the fuselage of a probable space vehicle. The radius of curvature at the stagnation point (r_n=0.20 m) is proper for the present tests; it is almost the same like that of the current space-plane SpaceLiner (Zuppardi *et al*. 2014). The dimensions of the computing dominion in the meridian plane (x, y) are: L_x=0.8 m, L_y=0.5 m.

The study relies on 24 runs: 2 entry trajectories (Mars, Earth), 4 altitudes (h=60, 70, 80, 90 km), 3 chemical conditions: 1) gas non-reactive and non-catalytic surface (NR), 2) gas reactive and non-catalytic surface (NC), 3) gas reactive and fully-catalytic surface (FC). Tables 1(a) and 1(b) report the input data to DS2V-4.5 64 bits for Mars and for Earth, respectively and the free stream Mach (M_∞), Reynolds ($Re_{D\infty}$), Knudsen ($Kn_{D\infty}$) numbers and the Reynolds number downstream a normal shock wave (Re_{D2}), for the aerodynamic characterization of the flow fields; D is the base diameter of the nose, D=0.72 m.

The free stream velocities for Mars and for Earth are those of a non-lifting capsule along the free orbital Earth re-entry and Mars entry, both ones already computed by Zuppardi and Savino (2015). As the radius of Mars (R_M=3.39×10^3 km) is about half than that of Earth (R_E=6.37×10^3 km), the orbital entry velocity for Mars is smaller than that for Earth. According to the Mars atmosphere model (NASA Glenn Research Center), temperature of Mars is much lower than that

Table 1(a) Input data and aerodynamic parameters: Mars

h [km]	V_∞ [m/s]	N_∞ [1/m^3]	T_∞ [K]	ρ_∞ [kg/m^3]	e_∞ [MJ/kg]	M_∞	$Re_{D\infty}$	$Kn_{D\infty}$	Re_{D2}
90	4667	3.08×10^{20}	50	2.21×10^{-5}	10.9	41.8	2.61×10^{4}	2.10×10^{-3}	149
80	4612	5.24×10^{20}	72	3.77×10^{-5}	10.7	34.4	3.11×10^{4}	1.45×10^{-3}	256
70	4506	9.86×10^{20}	94	7.09×10^{-5}	10.2	29.4	4.46×10^{4}	8.64×10^{-4}	490
60	4044	1.96×10^{21}	117	1.41×10^{-4}	8.2	23.7	6.67×10^{4}	4.67×10^{-4}	1015

Table 1(b) Input data and aerodynamic parameters: Earth

h [km]	V_∞ [m/s]	N_∞ [1/m^3]	T_∞ [K]	ρ_∞ [kg/m^3]	e_∞ [MJ/kg]	M_∞	$Re_{D\infty}$	$Kn_{D\infty}$	Re_{D2}
90	7700	7.12×10^{19}	187	3.39×10^{-6}	29.8	27.9	1.48×10^{3}	2.73×10^{-2}	37
80	7000	3.84×10^{20}	199	1.83×10^{-5}	24.6	24.7	6.91×10^{3}	5.12×10^{-3}	213
70	5933	1.72×10^{21}	220	8.21×10^{-5}	17.8	19.9	2.42×10^{4}	1.72×10^{-3}	1065
60	4624	6.44×10^{21}	247	3.07×10^{-4}	10.9	14.6	6.41×10^{4}	2.31×10^{-4}	4610

of Earth. The most relevant differences between the Mars and Earth trajectories are in the flow energy ($e_\infty=c_vT_\infty+V^2_\infty/2$) and in the Mach number; even though velocity is lower, due to lower temperature and therefore to lower sound speed, the Mach number for Mars is much higher than that for Earth. The flow energy e_∞ both for Earth and even more for Mars is lower than the ionization energy of Oxygen (e_{iO2}=36.4 MJ/kg) and of Carbon dioxide (e_{iCO2}=30.2 MJ/kg), therefore ionization has been not considered in the present computations.

The free stream Knudsen number ($Kn_{D\infty}$) and the Reynolds number behind a normal shock wave (Re_{D2}) indicate that both flow fields are in continuum low density regime. The transitional regime is defined, according to Moss (1995), in terms of the global Knudsen number by $10^{-3}<Kn_{D\infty}<50$ and, according to Vallerani (1973), in terms of the Reynolds number downstream a normal shock wave by $10^{-1}< Re_{D2} <10^{4}$.

The study of chemistry of the Mars atmosphere is not new; McKensie (1966) already dealt with this topic longer than 50 years ago. But, for the purpose of the present paper, the chemical model of the Mars atmosphere, proposed by Bird (2005) in the previous version 3.3 of the DS2V code, has been preferred and therefore implemented in the current version of the code. Both the McKensie and the Bird model considers the Mars atmosphere made up of 9 species (O_2, N_2, O, N, NO, C, CO, CO_2, AR) with molar fractions: X_{O2}=0.00176, X_{N2}=0.04173, X_{NO}=0.00014, X_C=0.00396, X_{CO}=0.00108, X_{CO2}=0.93399, X_{AR}=0.01734 constant with altitude. The McKensie model relies on 17 chemical reactions, the model reported by Bird is more complete. In fact, it relies on 54 chemical reactions: 40 dissociation, 7 forward exchange, 7 reverse exchange.

The Earth atmosphere is considered as made up of 5 species (O_2, N_2, O, N, NO). According to the US Standard atmosphere, air composition is practically constant in the altitude interval 60-90 km. The molar fractions are: X_{O2}=0.210, X_{N2}=0.790. The chemical model, built-in in the DS2V-4.5 64bits code is the Jos-Gupta-Thomson model (Gupta *et al.* 1989). This model relies on 23 chemical reactions: 15 dissociation, 2 forward exchange, 2 reverse exchange, 4 recombination.

Table 2 reports five surface recombination reactions, implemented in the present computations with the related exothermic molecular and specific energy. The conditions of non-catalytic and fully-catalytic surface are simulated by fixing to zero and to unit the probability for each surface recombination reaction, respectively.

Table 2 Surface recombination reactions and exothermic energy

Reaction	E [J]	e [MJ/kg]
$O+O->O_2$	8.20×10^{-19}	15.4
$N+N->N_2$	1.56×10^{-18}	33.6
$N+O->NO$	1.04×10^{-18}	20.9
$CO+O->CO_2$	7.25×10^{-19}	9.9
$C+O->CO$	1.78×10^{-18}	38.2

Table 3 Computation parameters

N_m	N_c	N_s	F_N
2.5×10^{7}	2.8×10^{6}	8.0×10^{4}	3.0×10^{9}

Table 4 Quality parameters of the DS2V runs

	Mars		Earth	
h [km]	mcs/λ	t_s/t_f	mcs/λ	t_s/t_f
90	0.04	12.9	0.004	15.9
80	0.06	15.8	0.02	12.5
70	0.11	14.4	0.10	15.0
60	0.22	10.0	0.40	8.8

4. Computation parameters and quality of the results

Tables 3 reports some computation parameters like the number of: Simulated molecules (N_m), collision (N_c) and sampling (N_s) cells, real molecules represented by each simulated molecule (F_N). These data are meaningful because roughly obtained in each computation. N_c and N_s were obtained by the adaptation procedure of the collision and sampling cells, using the numbers of molecules of 8 and of about 280 respectively, as suggested by DS2V-4.5 64bits.

The quality of the results can be verified from Table 4 reporting, at each altitudes of the two trajectories, the ratios mcs/λ, averaged over the collision cells and the ratios t_s/t_f: t_s is the simulation time, t_f is the time required to travel the length (L) of the body under study, in this case the nose (L=0.6 m, see Fig.1), at the free stream velocity: $t_f=L/V_\infty$.

Even though the ratio mcs/λ does not satisfy, at h=60 km of both trajectories, the optimal value of 0.2, however it is less than unit, as required by the DSMC method. The criterion of the stabilization of the computation, from a fluid-dynamic point of view, is also satisfied; a well known rule of thumb suggests considering a computation stabilized when the ratio t_s/t_f is O(10). Furthermore, the longer the simulation time the greater the beneficial effects on the quality of the results from a DSMC code. More specifically, the longer t_s, the larger the sample size on which the fluid-dynamic quantities are averaged during the evolution of the DSMC computation toward the steady state condition. Increasing the sample size, for making the average of the molecular properties, is equivalent to making a calculation with a larger number of molecules. Therefore, achieving a one to one correspondence between the real and the simulated molecules could be possible, thus the fluid-dynamic fluctuations match those in real gas. Finally, the jagging of the molecule time history profile is achieved in each computation.

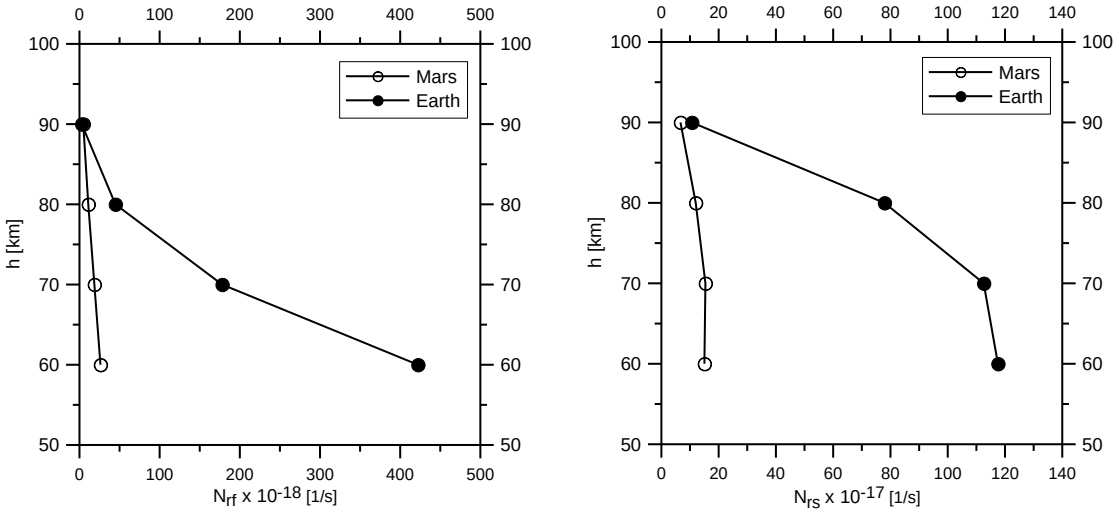

(a) (b)

Fig. 2 Profiles of number of reactions per second in the flow (a) and of number of reactions per second of fully-catalytic surface (b) as functions of altitude

Table 5 Fraction of reactions in the flow

	Mars		Earth	
h [km]	CO_2+CO_2-> CO_2+CO+O	CO_2+O-> $CO+O_2$	O_2+N_2->$2O+N_2$	O_2+N->$NO+O$
90	0.78	0.06	0.25	0.10
80	0.72	0.09	0.08	0.24
70	0.67	0.12	0.06	0.22
60	0.66	0.13	0.07	0.24

Table 6 Fractions of fully-catalytic surface reactions

	Mars		Earth	
h [km]	$O+O$->O_2	$C+O$->CO	$O+O$->O_2	$O+N$>NO
90	0.87	0.12	0.71	0.22
80	0.90	0.09	0.68	0.24
70	0.94	0.06	0.91	0.08
60	0.97	0.03	0.99	0.01

Table 4 reports, for each altitude and for each chemical condition, only one value of the parameters because roughly obtained in each computation at that altitude of the two trajectories. Thus, this value can be considered as representative of all corresponding computations.

5. Analysis of results

Figures 2(a) and 2(b) show the profiles of the number of reactions per second in the flow (N_{rf}, (a)) and the number of fully-catalytic surface reactions per second (N_{rs}, (b)) as functions of altitude

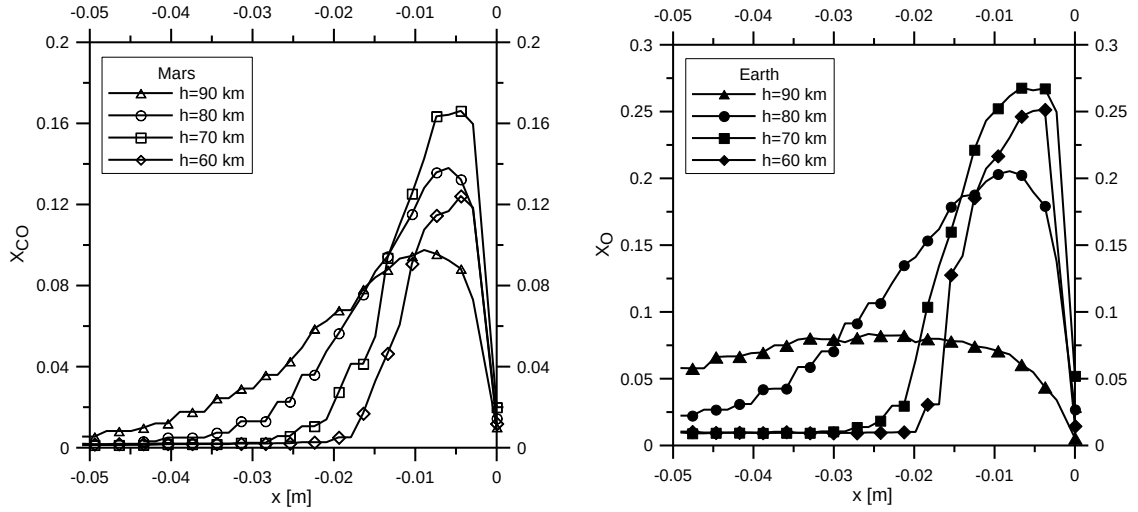

(a) (b)

Fig. 3 Profiles of molar fraction of CO and O in the shock layer for Mars (a) and for Earth (b)

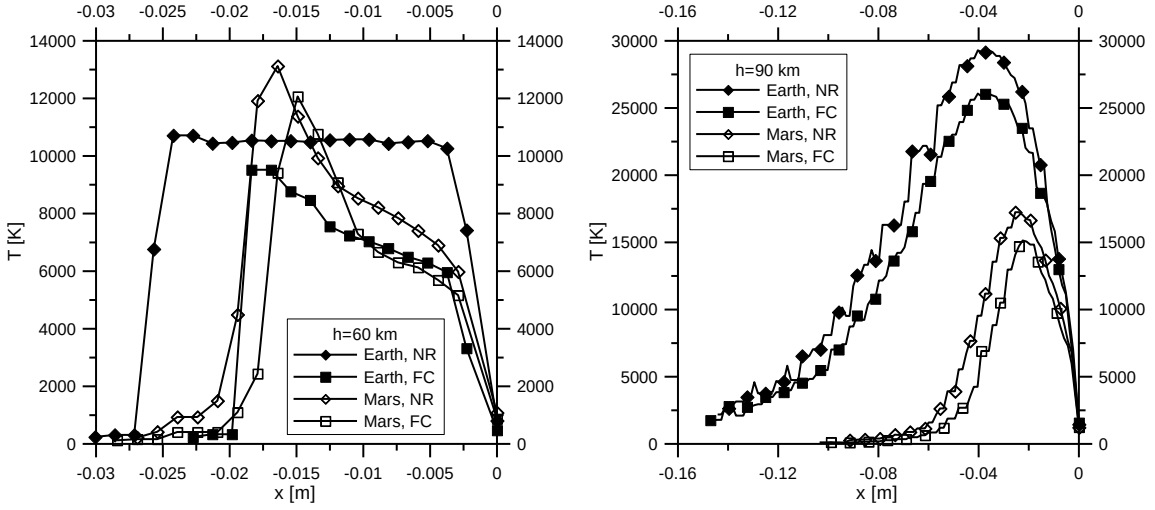

(a) (b)

Fig. 4 Profiles of temperature along the stagnation line at h=60 km (a) and at h=90 km (b)

for Mars and for Earth. As expected, both numbers of reactions decrease with increasing altitude or with decreasing density. Both numbers for Earth are higher than those for Mars; for example at h=60 km, N_{rf} and N_{rs} for Earth are 16.1 and 7.8 times higher than those for Mars. The higher values for Earth are due to higher density and/or to higher flow energy (see Tables 1(a) and 1(b)).

The two most likely chemical reactions are the dissociation reaction $CO_2+CO_2->CO_2+CO+O$ and the direct (endothermic) exchange reaction $CO_2+O->CO+O_2$ for Mars, the dissociation reaction $O_2+N_2->2O+N_2$ and the reverse (exothermic) exchange reaction $O_2+N->NO+O$ for Earth. Table 5 reports the fractions of the above reactions at the four altitudes. For the sake of completeness, Figs. 3(a) and 3(b) show the profiles, along the stagnation line in the shock layer, of the molar fractions of CO and O produced by dissociation of CO_2 and O_2 (computations have been

Table 7 Average temperature over the stagnation line and percentage variation

	Mars			Earth		
h [km]	$\overline{T}_{NR}$ [K]	$\overline{T}_{FC}$ [K]	$\frac{(\overline{T}_{NR}-\overline{T}_{FC})}{\overline{T}_{FC}}$%	$\overline{T}_{NR}$ [K]	$\overline{T}_{FC}$ [K]	$\frac{(\overline{T}_{NR}-\overline{T}_{FC})}{\overline{T}_{FC}}$%
90	6680	6214	7.5	15147	12758	18.7
80	6351	5489	15.7	10864	8820	23.2
70	4282	3245	32.0	11129	8037	38.5
60	6101	4458	36.9	8273	5524	49.8

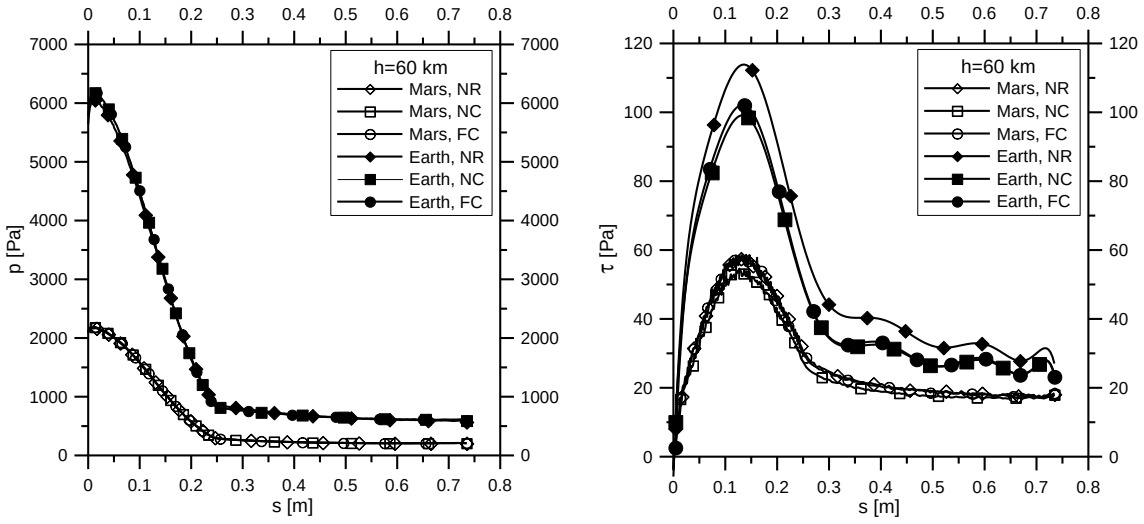

Fig. 5 Profiles of pressure (a) and skin friction (b) along the nose surface: h=60 km

carried out considering the nose surface as fully-catalytic). Table 6 reports the fractions of the fully-catalytic surface reactions. The surface recombination O+O->O_2 is the most likely equation also for Mars.

The effect of the endothermic reactions in the flow, both for Earth and for Mars, is higher than that of the exothermic reactions; this condition can be qualitatively evaluated by means of the profiles of temperature along the stagnation line in the shock layer (Fig.4(a) at h=60 km and Fig.4(b) at h=90 km). As expected, temperature computed considering the gas non reactive (and non-catalytic surface, NR) is higher than that computed considering the gas reactive (and fully-catalytic surface, FC). To quantify the chemical effects, Table 7 reports the values of temperature averaged over the shock layer, for non-reactive and reactive gas and the related percentage differences. Higher values of the percentage variation indicate that the influence of chemistry for Earth is higher than that for Mars and that this influence decreases with altitude.

The effects of chemistry are almost negligible on pressure and on skin friction and therefore on the aerodynamic drag. For example, Figs. 5(a) and 5(b) show the profiles of pressure and skin friction along the nose surface at the altitude of h=60 km; similar results were obtained also at higher altitudes. Fig.6 shows the profiles of the aerodynamic drag coefficient (C_D) of the nose as functions of altitude. The quantification of chemical condition on the drag coefficient is reported in Table 8; also the drag coefficient is almost independent from the chemical conditions. The very

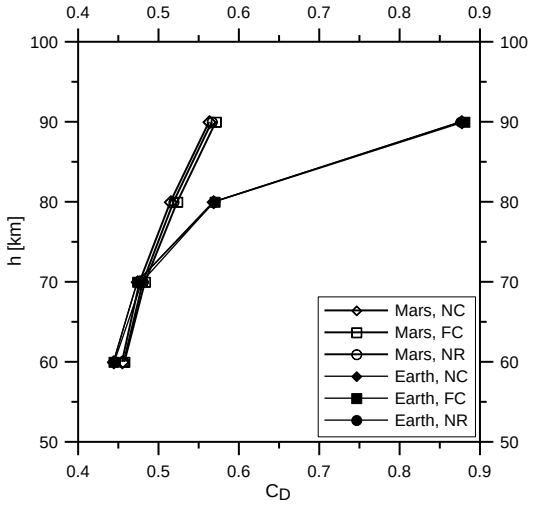

Fig. 6 Profiles of the drag coefficient of the nose as functions of altitude

Table 8 Percentage variations of drag coefficient

	Mars		Earth	
h [km]	$\frac{(C_{DNR}-C_{DFC})}{C_{DFC}}\%$	$\frac{(C_{DFC}-C_{DNC})}{C_{DNC}}\%$	$\frac{(C_{DNR}-C_{DFC})}{C_{DFC}}\%$	$\frac{(C_{DFC}-C_{DNC})}{C_{DNC}}\%$
90	-0.88	1.49	-0.57	0.42
80	-0.88	1.65	-0.11	0.30
70	-0.56	1.43	1.22	-0.04
60	-0.17	0.66	0.18	0.05

different values between the Mars and the Earth drag coefficients are due to the very different Reynolds and Mach numbers (see Tables 1(a) and 1(b)). For example, at h=90 km where the Reynolds number for Earth is about one order of magnitude smaller than that for Mars and the Mach number is less than half than that for Mars, C_D for Earth is about 0.88 and C_D for Mars is about 0.57; the percentage difference is about 54%.

On the opposite, the chemical effects are pretty consistent on heat flux. Figs. 7(a), 7(b) and Figs. 8(a), 8(b) show the heat flux profiles along the nose surface for Mars and for Earth at h=60 km (a) and at h=90 km (b) for each chemical condition. As expected, the values of heat flux, computed considering the gas non-reactive (and non-catalytic surface, NR), are the largest, the values of heat flux, computed considering the gas reactive (and non-catalytic surface, NC), are the smallest. Figures clearly show that the incidence of the chemical reactions decreases with altitude.

The profiles of heat flux at the nose stagnation point, as functions of altitude, are shown in Figs. 9(a) for Mars and 9(b) for Earth. In order to quantify the influence of the chemical reactions in the flow and on the surface, Table 9 reports, at each altitude, the percentage difference between the heat flux, computed considering the gas non-reactive (and non-catalytic surface, NR) and the heat flux, computed considering the gas reactive (and non-catalytic surface, NC). Similarly, the influence of the surface reactions is quantified by the percentage difference of heat flux, computed considering the gas reactive and fully-catalytic surface (FC) with respect to heat flux, computed considering the gas reactive and non-catalytic surface (NC). It seems that the influence of the

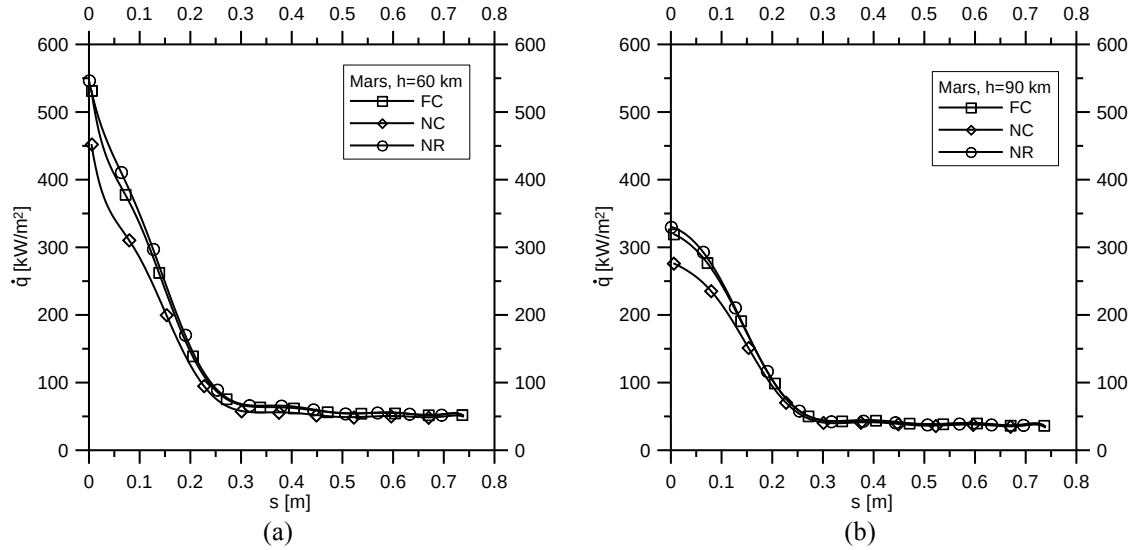

Fig. 7 Heat flux profiles along the body surface along the Mars entry at h=60 km (a) and at h=90 km (b)

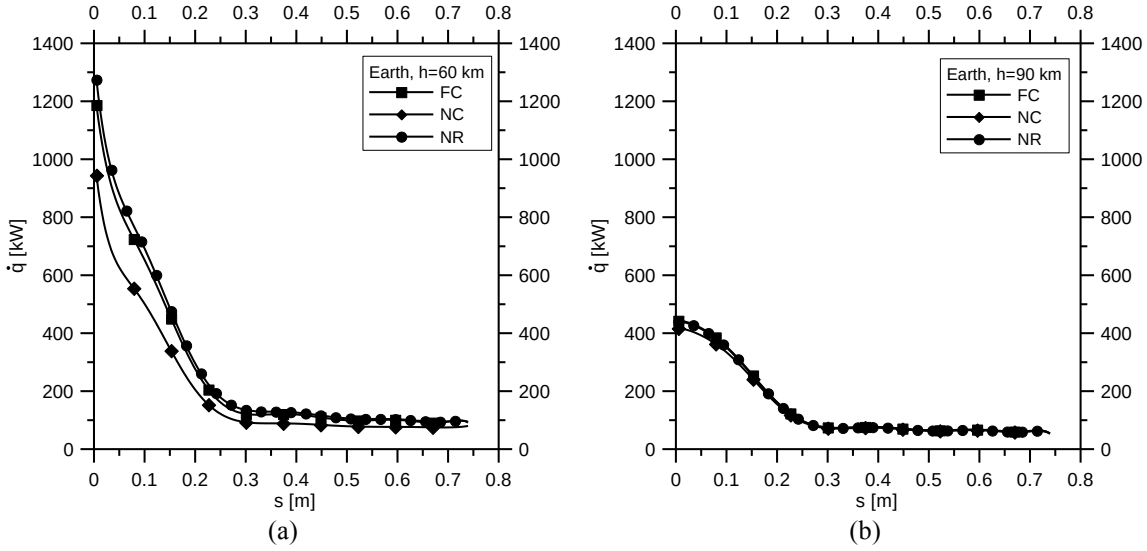

Fig. 8 Heat flux profiles along the body surface along the Earth re-entry at h=60 (a) and 90 km (b)

surface chemical condition, at the altitudes of 60, 70 and 80 k m is slightly higher for Earth. At 90 km both the flow and the surface reactions reduce; this reduction is slightly stronger for Earth. This is probably due to much stronger reduction of density; density reduces, from 80 and 90 km, of -41% for Mars and of -82% for Earth (see tables 1(a) and 1(b)).

6. Conclusions and further developments

The effects of chemical reactions both in the flow and on the surface of a test body, along the Mars entry and the Earth re-entry paths, have been quantified and compared. The Earth re-entry

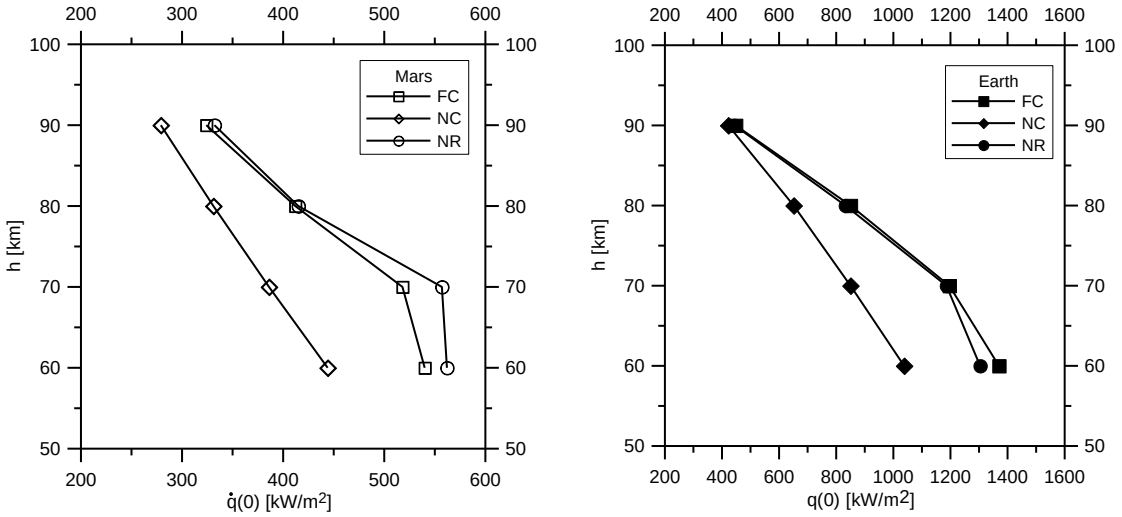

(a) (b)

Fig. 9 Stagnation point heat flux along the Mars entry (a) and Earth re-entry (b)

Table 9 Percentage variation of stagnation point heat flux

	Mars		Earth	
h [km]	$\frac{(\dot{q}_{NR}-\dot{q}_{NC})}{\dot{q}_{NC}}\%$	$\frac{(\dot{q}_{FC}-\dot{q}_{NC})}{\dot{q}_{NC}}\%$	$\frac{(\dot{q}_{NR}-\dot{q}_{NC})}{\dot{q}_{NC}}\%$	$\frac{(\dot{q}_{FC}-\dot{q}_{NC})}{\dot{q}_{NC}}\%$
90	19	16	5	6
80	25	24	28	31
70	44	34	40	41
60	27	22	26	32

velocity is higher than that of Mars entry therefore the flow is more energized, but the Mars atmosphere is almost made up of Carbon dioxide whose dissociation energy is lower than that of Oxygen; one could expect that the effects of chemistry on aerodynamic quantities are different from those along the Earth re-entry.

The study has been carried out computationally. Computer tests have been made in the altitude interval 60-90 km considering, as test body, an axial-symmetric nose of an aero-space-plane and as free stream velocities those of not-lifting capsules in free entry. As both flow fields are in transitional regime, the use of a DSMC code (DS2V-4.5 64 bits) has been mandatory.

At each altitude, three chemical conditions have been considered: 1) gas non reactive and non-catalytic surface, 2) gas reactive and non-catalytic surface, 3) gas reactive and fully-catalytic surface. Computations found that the numbers of reactions in the flow and on the surface in Earth re-entry are about one order of magnitude higher than those in Mars entry. Correspondingly, the effects of chemistry on the aerodynamic quantities in the shock layer, as per temperature, are higher for Earth. The influence of surface reaction was negligible on pressure and on skin friction, therefore on aerodynamic drag, but it was consistent on heat flux.

The present study is not exhaustive therefore further computer tests are needed. Tests at other altitudes, as well as considering other possible entry trajectories, have been scheduled. More specifically, interplanetary or direct entry trajectories will be considered. In fact, this kind of

entry/re-entry is characterized by much higher velocity therefore by much higher energy. For example, velocity at h=90 km is about 11 km/s for Earth re-entry and about 5 km/s for Mars entry.

References

Barbato, M. and Bruno, C. (1996), "Heterogeneous catalysis: Theory, models and applications", *Molecular Physics and Hypersonic Flows*, 139-160, Springer, Netherlands.

Bird, G.A. (2006), "Sophisticated versus simple DSMC", *Proceedings of the 25th International Symposium on Rarefied Gas Dynamics*, Saint Petersburg, Russia, July.

Bird, G.A. (1998), *Molecular Gas Dynamics and Direct Simulation Monte Carlo Method*, Clarendon Press, Oxford, United Kingdom.

Bird, G.A. (2005), "Visual DSMC program for two-dimensional flows"*, DS2V Program User's Guide*, Ver. 3.3, G.A.B. Consulting Pty Ltd., Sydney, Australia.

Bird, G.A. (2012), "Visual DSMC program for two-dimensional flows", *DS2V Program User's Guide*, Ver. 4.5, G.A.B. Consulting Pty Ltd., Sydney, Australia.

Bird, G.A. (2013), *The DSMC method*, Ver. 1.1, CreateSpace Independent Publishing Platform, California, U.S.A.

Bird, G.A., Gallis, M.A., Torczynski, J.R. and Rader, D.J. (2009), "Accuracy and efficiency of the sophisticated direct simulation Monte Carlo algorithm for simulating non-continuum gas flows", *Phys. Fluids,* **21**(1), 017103.

Gallis, M.A., Torczynski, J.R., Rader, D.J. and Bird, G.A. (2009), "Convergence behavior of a new DSMC algorithm", *J. Comput. Phys.*, **228**(12), 4532-4548.

Gupta, R.N., Yos, J.M. and Thompson, R.A. (1989), "A review of reaction rates and thermodynamic transport properties for an 11-species air model for chemical and thermal non-equilibrium calculations to 30,000 K", NASA-RP-1232; NASA Langley Research Center, U.S.A.

Hao, J., Wang, J., Gao, Z. and Jiang, C. (2017), "Comparison of transport properties models for numerical simulation of Mars entry vehicles", *Acta Astronautica*, **130**, 24-33.

Hollis, B.R. and Prabhu, D.K. (2013), "Assessment of laminar, convective aeroheating prediction uncertainties for Mars entry vehicles", *J. Spacecraft Rockets*, **50**(1), 56-68.

Kolesnikov, A.F., Gordeev, A.N. and Vasilevskii, S.A. (2016), "Effects of catalytic recombination on the surface of metals and quartz for the conditions of entry into the Martian atmosphere", *High Temp.*, **54**(1), 29-37.

McKensie, R.L. (1966), "An estimate of the chemical kinetics behind normal shock waves in mixtures of carbon dioxide and nitrogen for conditions typical of Mars entry", NASA-TN-D-3287; NASA Ames Research Center, U.S.A.

Moss, J.N. (1995), "Rarefied flows of planetary entry capsules", *Special Course on "Capsule aerothermodynamics"*, Rhode-Saint-Genèse, Belgium, May.

NASA Glenn Research Center (2015), Mars Atmosphere Model; NASA Glenn Research Center, Cleveland, U.S.A., www.grc.nasa.gov/www/k-12/airplane/atmosmrm.html.

Reynier, P. (2014), "Survey of aerodynamics and aerothermodynamics efforts carried out in the frame of Mars exploration projects", *Prog. Aerosp. Sci.*, **70**, 1-27.

Shen, C. (2005), *Rarefied Gas Dynamic: Fundamentals, Simulations and Micro Flows*, Springer-Verlag, Berlin, Germany.

Vallerani, E. (1973), "A review of supersonic sphere drag from the continuum to the free molecular flow regime", *Proceedings of the 41st AGARD Conference*, London, United Kingdom, April.

Wang, X., Yan, C., Zheng, W., Zhong, K. and Geng, Y. (2016), "Laminar and turbulent heating predictions for Mars entry vehicles", *Acta Astronautica*, **128**, 217-228.

Yang, X., Tang, W., Gui, Y., Du, Y., Xiao, G. and Liu, L., (2014), "Hypersonic static aerodynamics for Mars science laboratory entry capsule", *Acta Astronautica*, **103**, 168-175.

Zuppardi, G. (2015), "Aerodynamic control capability of a wing-flap in hypersonic, rarefied regime", *Adv.*

Aircraft Spacecraft Sci., **2**(1), 45-56.
Zuppardi, G. (2018), "Effects of SWBLI and SWSWI in Martian atmosphere entry", *Proceedings of 31st International Symposium on Rarefied Gas Dynamics*, Glasgow, United Kingdom, July.
Zuppardi, G., Morsa, L., Sippel, M. and Schwanekamp, T. (2014), "Aero-thermo-dynamic analysis of the SpaceLiner-7.1 vehicle in high altitude flight", *Proceedings of the 29th International Symposium on Rarefied Gas Dynamics*, Xian, China, July.
Zuppardi, G. and Savino, R. (2015), "DSMC aero-thermo-dynamic analysis of a deployable capsule for Mars entry", *A Paper Presented at DSMC15 Symposium*, Kapaa, Hawaii, U.S.A., September.

EC